

*Letter to the Editor***Chandra measurement of the geometrical distance to Cyg X-3 using its X-ray scattering halo**P. Predehl¹, V. Burwitz¹, F. Paerels², and J. Trümper¹¹ Max-Planck-Institut für Extraterrestrische Physik, Giessenbachstrasse, 85748 Garching, Germany (predehl@mpe.mpg.de)² Columbia University, New York, USA

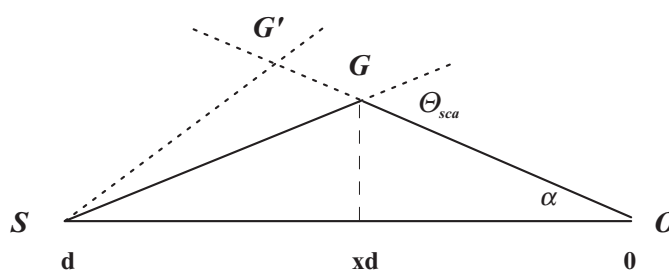
Received 24 March 2000 / Accepted 8 April 2000

Abstract. Using Chandra-HETGS data of Cyg X-3 we succeeded for the first time in applying a method, developed 27 years ago, to directly determine the geometric distance to X-ray sources. The method implies the existence of a halo of radiation scattered on interstellar dust. Any intensity variations of the source itself appear delayed and smeared out in the halo. By analysing and correlating the X-ray lightcurves at different radial distances from the source, we could determine the distance to Cyg X-3 to be approximately 9 kpc. Even though the statistics in this dataset are meager the usefulness and the possibilities of this method are convincingly demonstrated.

Key words: scattering – stars: binaries: eclipsing – ISM: clouds – X-rays: galaxies – X-rays: ISM

1. Introduction

The interaction of X-rays with interstellar dust grains leads not only to mere absorption but also to small angle scattering. Therefore, X-ray sources behind sufficiently large dust columns are surrounded by haloes of faint and diffuse radiation. This effect and its use as a powerful diagnostic tool was first described theoretically by Overbeck (1965), the first detection of an X-ray halo almost 20 years later was reported by Rolf (1983). Mauche & Gorenstein (1986) showed that the shape and strength of the haloes as derived from their measurements with the Einstein Observatory were consistent with common grain models, e.g., the one established by Mathis et al. (1977). The up to now most complete investigation on scattering haloes was done by Predehl & Schmitt (1994) based on observations with ROSAT from both the all-sky survey as well as a number of pointed observations. They found a strong correlation between the strength of haloes (or the optical depth in scattering, respectively), the X-ray absorption and the visual extinction for X-ray sources with known optical counterparts. These relations provide a precise differ-

**Fig. 1.** Scattering geometry

entiation between interstellar and local matter: both extinction and X-ray absorption are produced by the *total* column density between source and observer, the scattering, however, only by dust on large scales, i.e., the ISM.

Scattered radiation has to travel along a slightly longer path than the direct, unscattered light. Any intensity variation of the source therefore occurs somewhat delayed in the halo. Trümper and Schönfelder (1973) proposed a method for using this behaviour to measure the distance to variable X-ray sources. Although it was presented almost 30 years ago, this method could never be applied so far. The main reason is that the amplitude and the timescale of the intensity variation together with the distance of the source have to fit the angular resolution of the observing instrument. Using instruments with moderate angular resolution, the presence of scattering haloes has only a damping effect on the measured intensity variation. These observational aspects are discussed by, e.g., Molnar & Mauche (1986) and Kitamoto et al. (1989).

The attractiveness of the ‘halo-method’ is that it yields a *geometrical* rather than an *physical* distance from other methods like the 21 cm absorption, visual extinction, or X-ray absorption. A good example for a wrong distance estimate is for Sco X-1 which was assumed to be at a distance between 25 and 1000 pc until Bradshaw et al. (1997) obtained a distance of 2.8 kpc from VLBI measurements thus placing it far outside the galactic dust and gas layer.

Send offprint requests to: P. Predehl

In this paper we present, to our knowledge for the first time, a successful application of this distance determination method. Using data taken with the Chandra X-ray Observatory, we could measure the approximate distance to Cyg X-3. This object is an eclipsing X-ray binary with an orbital period of 4.8 hours (Brinkman et al. 1972).

2. Delays of scattered radiation

According to Fig. 1 light travels either along the direct path between the X-ray source S and the observer O (distance d) or can take a ‘detour’ via a dust grain G (by scattering). x denotes the fractional distance where the scattering takes place, α the angle of observation and Θ_{sca} the scattering angle. For details on X-ray scattering on interstellar dust, the related physics and the observational aspects and limits we refer to the work done by Hayakawa (1970), Mathis & Lee (1991), and Predehl & Klose (1996). For the purpose here it is only relevant to note that the differential scattering cross section depends on the scattering angle Θ or the observing angle α , respectively, the photon energy E , and the grain size a according to

$$\frac{d\sigma}{d\Omega} \sim e^{-0.46E^2 a^2 \frac{\alpha^2}{(1-x)^2}} \quad (1)$$

with α given in arcmin, a in μm , E in keV. The total scattering cross section depends on the photon energy according to

$$\sigma_{\text{sca}} \sim E^{-2} \quad (2)$$

The optical depth in scattering τ_{sca} is defined as the product of σ_{sca} and the grain column density along the line of sight N . The relative halo strength is given by

$$I_{\text{halo}} = 1 - e^{-\tau_{\text{sca}}} \quad (3)$$

The time delay dt of a scattered photon with respect to an unscattered one is given by (see Fig. 1):

$$dt = \frac{d}{2c} \frac{x\alpha^2}{1-x} = 1.15 d \frac{x\alpha^2}{1-x} \quad (4)$$

if d is given in kpc and α in arcsec (c is the speed of light).

The halo radiation is composed of scattering anywhere along the line of sight, thereby producing different time delays (Eq. 4). Since the scattering is generally a strong function of the scattering angle (Eq. 1), the halo is produced preferentially by grains close to the observer. However, for the observing angles α relevant for this study (~ 10 arcsec, see below) together with a mean grain size $a = 0.1 \mu\text{m}$ and photon energies below 2 keV, the differential cross section is constant over about 95% of the line of sight. Therefore, we can handle the delay effects within the scattering halo using Eq. 4 alone.

3. Observation and data analysis

Cyg X-3 was observed with the High Energy Transmission Grating Spectrometer (HETGS, see Markert et al. 1994 for a description) on board of Chandra on October 20, 1999, with a total

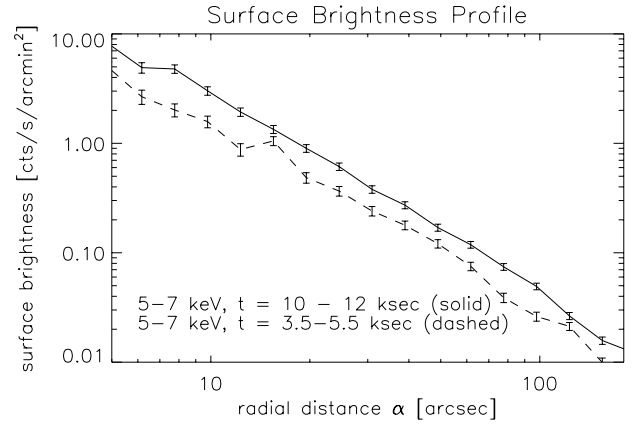


Fig. 2. Radial surface brightness profile of Cyg X-3 within the 5–7 keV energy band measured at the maximum of the lightcurve (10–12 ksec after begin of the observation, solid line) and during the minimum (3.5–5.5 ksec, dashed line)

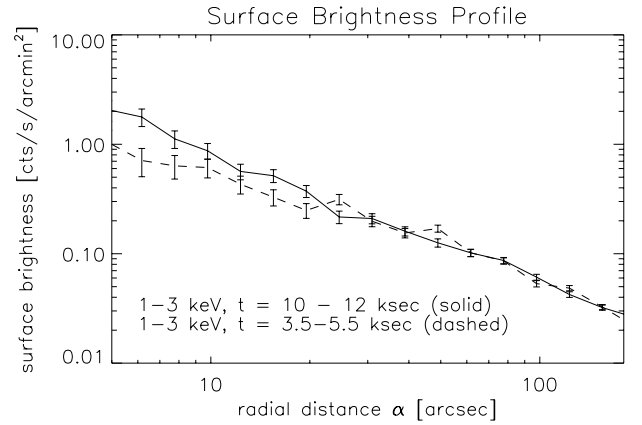


Fig. 3. Same as Fig. 2 but for photon energies in 1 to 3 keV range.

exposure time of 12.3 ksec, starting at 01:11:38 UT. The observation covered the binary phases from -0.3 to $+0.4$. Therefore the broad minimum of the lightcurve is found at the centre of our observation. The primary goal of the observation was an investigation of the emission spectrum of Cyg X-3 (Paerels et al. 2000). For the present study, we have used the non-dispersed (zeroth order) events only. The use of the grating reduced the countrate by a factor of four compared with a pure imaging observation. Nevertheless, Cyg X-3 is strong enough for producing pile-up effects within the innermost 1 arcsec. The dispersed spectra as well as the ‘out-of-time’ events of the strong point source, i.e., those events recorded while reading out the CCD-detector, were cut out by applying a spatial filter which, in azimuth around the centroid of the source covers a total of 68° . This reduced the number of events used in this analysis by another 19%.

The extraction of a dust scattering halo has to rely on a careful subtraction of the instrumental point response function (PSF) which, at larger radii, is produced by scattering off the mirror surface. The amount of the mirror scattering increases towards higher energies, unlike the scattering on interstellar dust (see

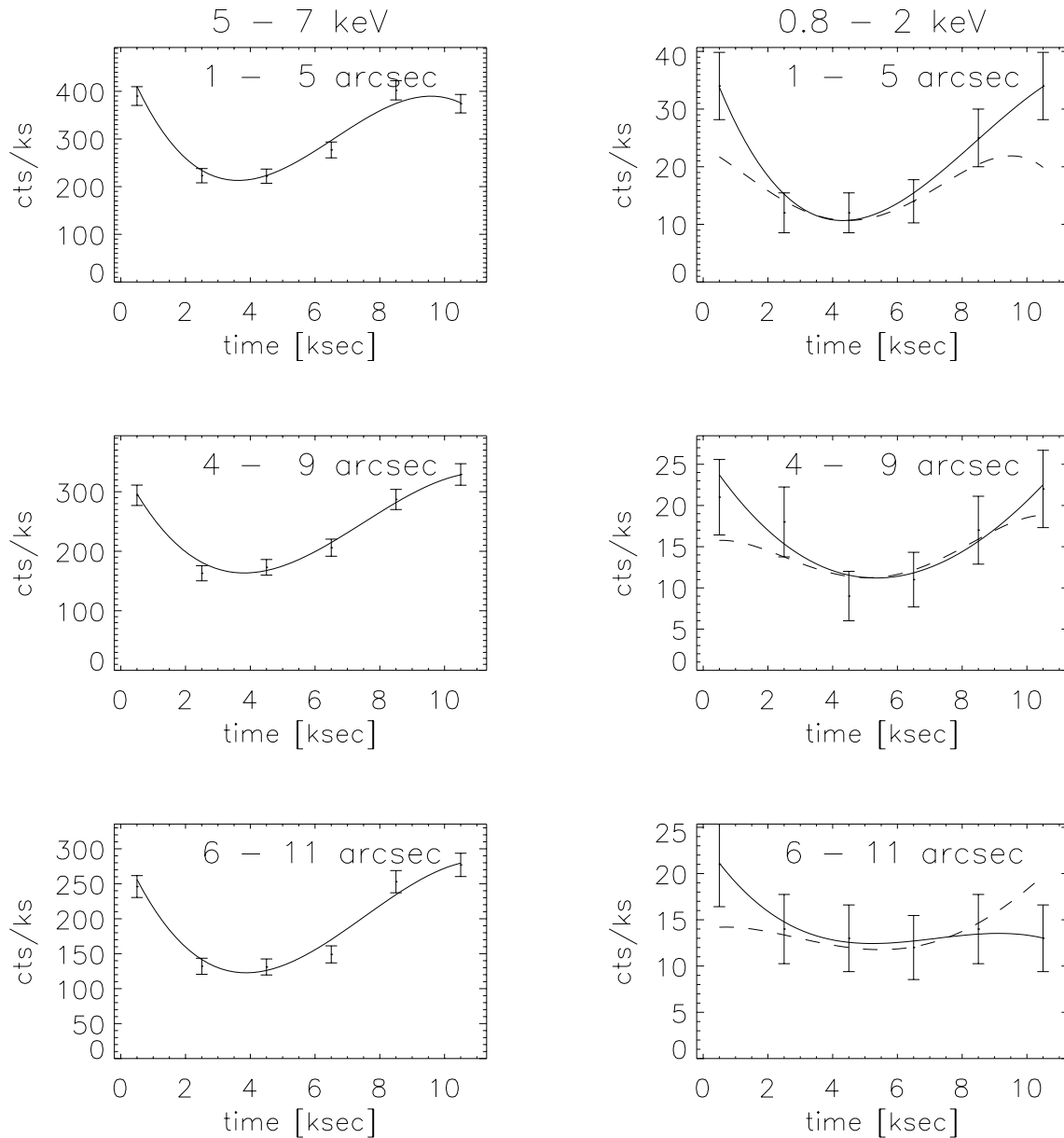


Fig. 4. Lightcurves of Cyg X-3 at energies between 5 and 7 keV (left plots) and between 0.8 and 2 keV (right plots). Events are taken from different annuli (from top): 1–5 arcsec, 4–9 arcsec, 6–11 arcsec. Solid lines are third-order polynomial fits to the data, dashed lines (right) are fits to ‘delayed’ high-energy lightcurves. From these fits, a distance of Cyg X-3 of 9 kpc is determined.

Eq. 2). Therefore one expects that the radial surface brightness profile around a source to be dominated in its inner part by the PSF alone, in the outer parts either by the dust scattering (at low energies) or by mirror scattering (at high energies). This behaviour is reflected in Figs. 2 and 3: at energies between 5 and 7 keV, intensity variations of the sources can be seen at all radial distances. In contrast, below 2 keV these variations disappear at radial distances greater than about 20 arcsec because the delay of the radiation scattered on interstellar dust becomes comparable with or larger than the timescales of the intrinsic intensity variations (4.8 h). Those are not only delayed but also smeared out because the delay is connected with the dust distri-

bution along the line of sight (Eq. 4). A simple estimate using Eq. 4 with a mean value $x = 0.5$ of equally distributed dust along the line of sight gives a distance of Cyg X-3 of about 10 kpc. Dickey (1983) has found a lower limit of 9.2 kpc¹ using 21 cm wavelength absorption data, Predehl & Schmitt 1994 derived 8 kpc as distance *through the galactic dust layer* from their comparison of X-ray scattering and absorption.

¹ Dickey’s finding was given as: $D = 11.6(\pi_{\odot}/10 \text{ kpc}) \text{ kpc}$ with π_{\odot} is the Galactic Centre distance which, at that time, was assumed to be 10 kpc. We have adopted a value of 8 kpc (Genzel, private communication).

In order to check this result independently and more precisely, we have constructed lightcurves within different energy bands and annuli of different radii around the source (Fig. 4). At energies between 5 and 7 keV, the total halo intensity is reduced by more than a factor of ten compared with the lowest possible energy range of 0.8 to 2 keV (Eq. 2). Here, the low energy limit is given by the interstellar absorption, the upper limit is chosen in order to get sufficient photon statistics. As expected, the lightcurve in the 5 to 7 keV band is independent of the annulus selected. Even at radial distances $\alpha = 50$ arcsec (not shown here) it remains almost unchanged. In contrast, in the low energy band, where the scattering halo dominates, the lightcurve is shifted by the time delays of the scattered radiation and is also damped.

In a second step, we have made a Monte Carlo simulation using the data itself: the high energy events (which reflect the intrinsic source variability) were ‘delayed’ by a simulated scattering on interstellar dust which was assumed to be uniformly distributed between source and observer. Using Eq. 4, the distance was varied until we got a match between real and simulated lightcurves (dashed lines in Fig. 4). A problem arose from the fact that the observation was shorter than one orbital cycle. This leads to distortions at both ends of the lightcurve if the delays became comparable with the duration of the orbital period. As a result of this exercise, we have determined the distance $d = 9_{-2}^{+4}$ kpc to Cyg X-3.

4. Conclusion

Using Chandra-HETGS data of Cyg X-3, we have analysed the lightcurves at different radial distances from the source. While at higher energies the lightcurve remains unchanged, at low energies it varies strongly within the inner 10-15 arcsec until all intensity variations completely vanish beyond about 20 arcsec. This effect can be interpreted as the result of light that is scattered by dust having to travel a longer distance to the observer. The resulting additional time causes the (intrinsic) lightcurve also to be delayed and smeared out. From the measured delays, the distance of the source could be determined to be approximately 9 kpc. The distance obtained here is consistent with those obtained using other methods. However, the ability of the method, particularly when using Chandra with its high angular resolution, could be convincingly demonstrated, despite of the statistical uncertainties inherent in the present observation.

The observation was, unfortunately, shorter than a complete 4.8 h orbital cycle of Cyg X-3, and the countrate was reduced by a factor of four because the grating was inserted and most of the radiation was blocked or dispersed. Limited by the low quality of the data, the result could not be improved even when using the real dust distribution (if it were known) rather than our simplified model. The simple model leads to wrong results only for the case of an extreme dust distribution, e.g. if all the dust were concentrated in a ‘thin layer’ near the source. This would produce a relatively weak halo due to the large scattering angles involved. However, the ratio between optical depth in scattering and X-ray absorption for Cyg X-3 is in agreement with the general law (Predehl and Schmitt 1994) excluding such an extreme dust distribution. Actually we note that a longer observation covering 2 to 3 orbital periods, of course without the grating, would allow not only a more precise distance measurement but in principle also a determination of the dust distribution along the line of sight.

Acknowledgements. Part of this work was supported by the DLR (Deutsches Zentrum für Luft- und Raumfahrt) under contract no. 50 OX 0001.

References

- Bradshaw C.F., Fomalont E.B., Geldzahler B.J., 1997, ApJ 484, L55
 Brinkman A.C., Parsignault D., Giacconi R., Gursky H., Kellogg E., Schreier E., Tananbaum H., 1972, IAU Circ. 2446
 Dickey J.M., 1983 ApJ 273, L71
 Hayakawa S., 1970, Prog. Theor. Phys. 43, 1224
 Kitamoto S., Miyamoto S., Yamamoto T., 1989 Publ. Astron. Soc. Japan 41, 81
 Markert T.H., Canizares C.R., Dewey D., McCuirk M., Pak C., Schatzenburg M.L., 1995, Proc. SPIE 2280, 168
 Mauche C. W., Gorenstein P., 1986, ApJ 302, 371
 Mathis J.S., Lee C.-W., 1991, ApJ 376, 490
 Mathis J. S., Rumpl W., Nordsieck K. M., 1977, ApJ 217, 425
 Molnar L.A., Mauche Ch. W., 1986, ApJ 310, 343
 Overbeck J.W., 1965, ApJ 141, 864
 Paerels F., Cottam J., Sako M., Liedahl D.A., Brinkman A.C., van der Meer R.L.J., Kaastra J.S., Predehl P., 2000 ApJ accepted
 Predehl P., Klose S., 1996, A&A 306, 283
 Predehl P., Schmitt J.H.M.M., 1994 A&A 293, 889
 Rolf D.P., 1983, Nature 302, 46
 Trümper J., Schönfelder V., 1973 A&A 25, 445